

- McRae, B. J., Kurachi, K., Heimark, R. L., Fujikawa, K., Davie, E. W., & Powers, J. C. (1981) *Biochemistry* 20, 7196-7206.
- Meyer, E., Cole, G., Radhakrishnan, R., & Epp, O. (1988) *Acta Crystallogr. B* 44, 26-38.
- Murphy, M. E. P., Moulton, J., Bleackley, R. C., Gershenfeld, H., Weissman, I. L., & James, M. N. G. (1988) *Proteins: Struct., Funct., Genet.* 4, 190-204.
- Oleksyszyn, J., & Powers, J. C. (1989) *Biochem. Biophys. Res. Commun.* 161, 143-149.
- Podack, E. R. (1986) *J. Cell. Biochem.* 30, 133-138.
- Podack, E. R., Young, J. D.-E., & Cohn, Z. A. (1985) *Proc. Natl. Acad. Sci. U.S.A.* 82, 8629-8633.
- Poe, M., Bennett, C. D., Biddison, W. E., Blake, J. T., Norton, G., Sigal, N. H., Rodkey, J. A., Turner, R. V., Wu, J. K., & Zweerink, H. J. (1988) *J. Biol. Chem.* 263, 13215-13222.
- Poe, M., Blake, J. T., Boulton, D. A., Gammon, M., Sigal, N. H., Wu, J. K., & Zweerink, H. J. (1991a) *J. Biol. Chem.* 266, 98-103.
- Poe, M., Wu, J. K., Blake, J. T., Zweerink, H. J., & Sigal, N. H. (1991b) *Arch. Biochem. Biophys.* 284, 215-218.
- Powers, J. C. (1977) *Chemistry and Biochemistry of Amino Acids, Peptides and Proteins* (Weinstein, B., Ed.) Vol. 4, pp 65-178, Marcel Dekker, New York.
- Powers, J. C., & Harper, J. W. (1986) *Proteinase Inhibitors* (Barrett, A. J., & Salvensen, G. S., Eds.) pp 55-152, Elsevier Science Publishers, Amsterdam/New York.
- Powers, J. C., Kam, C.-M., Narasimhan, L., Oleksyszyn, J., Hernandez, M. A., & Ueda, T. (1989) *J. Cell. Biochem.* 39, 33-36.
- Redelman, D. D., & Hudig, D. (1980) *J. Immunol.* 124, 870-878.
- Schechter, I., & Berger, A. (1967) *Biochem. Biophys. Res. Commun.* 27, 157-162.
- Simon, M. M., Hoschutzky, H., Fruth, U., Simon, H.-G., & Kramer, M. D. (1986) *EMBO J.* 5, 3267-3274.
- Tanaka, T., Minematsu, Y., Reilly, C. F., Travis, J., & Powers, J. C. (1985) *Biochemistry* 24, 2040-2047.
- Tschopp, J., & Nabholz, M. (1990) *Annu. Rev. Immunol.* 8, 279-302.
- Tschopp, J., Masson, D., & Stanley, K. K. (1986) *Nature (London)* 322, 831-834.
- Ueda, T., Kam, C.-M., & Powers, J. C. (1990) *Biochem. J.* 265, 539-545.
- Young, J. D.-E., Hengartner, H., Podack, E. R., & Cohn, Z. A. (1986a) *Cell* 44, 849-859.
- Young, J. D.-E., Podack, E. R., & Cohn, Z. (1986b) *J. Exp. Med.* 164, 144-155.
- Young, J. D.-E., Cohn, Z. A., & Podack, E. R. (1986c) *Science* 233, 184-190.
- Young, J. D.-E., Liu, C.-C., Leong, L. G., & Cohn, Z. A. (1986d) *J. Exp. Med.* 164, 2077-2082.
- Young, J. D.-E., Leong, L. G., Liu, C.-C., Damiano, A., Wall, D. A., & Cohn, Z. A. (1986e) *Cell* 47, 183-194.

Crystal Structure of Unliganded *Escherichia coli* Dihydrofolate Reductase. Ligand-Induced Conformational Changes and Cooperativity in Binding^{†,‡}

Christopher Bystroff[§] and Joseph Kraut^{*}

Department of Chemistry, University of California, San Diego, La Jolla, California 92093

Received July 3, 1990; Revised Manuscript Received October 24, 1990

ABSTRACT: The crystal structure of unliganded dihydrofolate reductase (DHFR) from *Escherichia coli* has been solved and refined to an *R* factor of 19% at 2.3-Å resolution in a crystal form that is nonisomorphous with each of the previously reported *E. coli* DHFR crystal structures [Bolin, J. T., Filman, D. J., Matthews, D. A., Hamlin, B. C., & Kraut, J. (1982) *J. Biol. Chem.* 257, 13650-13662; Bystroff, C., Oatley, S. J., & Kraut, J. (1990) *Biochemistry* 29, 3263-3277]. Significant conformational changes occur between the apoenzyme and each of the complexes: the NADP⁺ holoenzyme, the folate-NADP⁺ ternary complex, and the methotrexate (MTX) binary complex. The changes are small, with the largest about 3 Å and most of them less than 1 Å. For simplicity a two-domain description is adopted in which one domain contains the NADP⁺ 2'-phosphate binding site and the binding sites for the rest of the coenzyme and for the substrate lie between the two domains. Binding of either NADP⁺ or MTX induces a closing of the PABG-binding cleft and realignment of α -helices C and F which bind the pyrophosphate of the coenzyme. Formation of the ternary complex from the holoenzyme does not involve further relative domain shifts but does involve a shift of α -helix B and a floppy loop (the Met-20 loop) that precedes α B. These observations suggest a mechanism for cooperativity in binding between substrate and coenzyme wherein the greatest degree of cooperativity is expressed in the transition-state complex. We explore the idea that the MTX binary complex in some ways resembles the transition-state complex.

This is the second of two crystallographic papers describing substrate binding and induced conformational changes in

Escherichia coli dihydrofolate reductase (DHFR).¹ The previous paper (Bystroff et al., 1990) reported the structures of the NADP⁺ holoenzyme and the folate-NADP⁺ ternary

[†] Based on the Ph.D. Dissertation of C.B.; supported by NIH Grant CA 17374.

[‡] Coordinates for the apo-dihydrofolate reductase described have been deposited in the Brookhaven Protein Data Bank under 5DFR.

^{*} Author to whom correspondence should be addressed.

[§] Present address: Department of Biochemistry and Biophysics, University of California, San Francisco, CA 94143-0448.

¹ Abbreviations: ABD, adenosine binding domain; DHFR, dihydrofolate reductase; MTX, methotrexate; NADP⁺ and NADPH, nicotinamide adenine dinucleotide phosphate (oxidized and reduced, respectively); NMN, nicotinamide mononucleotide; PABG, (*p*-aminobenzoyl)glutamate.

complex. With the apoenzyme structure described here and the earlier methotrexate (MTX) binary complex (Bolin et al., 1982; Filman et al., 1982), we now have an *E. coli* DHFR structure for every combination of occupied or unoccupied substrate and cofactor binding sites. In our previous paper we presented a static picture of the binding interactions between enzyme and ligands, setting aside discussion of conformational changes in the enzyme. In this paper we introduce the structure of the unliganded enzyme molecule and explore conformational changes induced by the binding of MTX, NADP⁺, and folate. We suggest how conformational changes in DHFR may transmit cooperativity between parts of ligands that are not in direct contact with each other. Finally, we will explore the possibility that the unusually tight binding of MTX in the binary complex ($K_d = 0.6$ nM; Appleman et al., 1988) is due in part to an enzyme conformation which resembles the conformation of the enzyme in the transition state.

This crystallographic study of conformational variability in *E. coli* DHFR follows numerous solution studies on the subject. Stopped-flow and steady-state kinetics, ¹H NMR, ¹³C NMR, ³¹P NMR, and the use of fragments or analogues of the substrates are among the techniques that detect changes in enzyme conformation. The data indicate that the apoenzyme exists in at least two conformations with distinct cofactor, substrate, and inhibitor binding affinities and that one of these conformers is kinetically inactive (Pattishall et al., 1976; Cayley et al., 1981; Penner & Frieden, 1985; Appleman et al., 1990). Additionally, the folate-NADP⁺ ternary complex appears to exist in at least three conformations (Birdsall et al., 1981a,b). And conformational changes have been invoked to explain the slow, tight binding of MTX (Williams et al., 1980) as well as cooperativity in binding between fragments of the MTX molecule (Birdsall et al., 1978). Despite all of these findings, however, the nature and mechanics of these putative conformational changes in DHFR have largely remained a mystery. In this paper we present a detailed view of ligand-induced conformational changes in *E. coli* DHFR as seen by X-ray crystallography in the hope of providing a firmer structural basis for thinking about these questions.

MATERIALS AND METHODS

Crystallization Conditions. *E. coli* DHFR was purified and stored as described by Bystroff et al. (1990). Large single crystals of apo-DHFR were grown at 4 °C from solutions of 24 mg/mL unliganded protein in pH 5.4 50 mM sodium/potassium phthalate to which was added 50% (w/w) PEG6000 (BDH) at a ratio of 1:9. Hanging or sitting drops of approximately 10 μ L were vapor diffused against 25% PEG6000. Crystals grew without seeding on only two occasions, once after 2 days and once after more than a month. Crystals could be reproduced by touch seeding² after 1–2 days of equilibration and grew to full size within 1 day after seeding. The best crystals grew to $1.0 \times 0.5 \times 0.5$ mm. Precession films revealed space group $P3_121$ or $P3_221$ and unit-cell dimensions $a = b = 68.7$ Å and $c = 83.4$ Å.

Data Collection. X-ray intensity data were collected on the Mark 2 multiwire area detector in the laboratory of Xuong and co-workers. A total of 63 697 observations on 14 169 out of a possible 14 730 reflections to 2.05 Å were obtained in 18 h at room temperature. After four cycles of semiautomatic

rejection of outlying observations, the merging R factor was 4.3% for all reflections. Merging R factors for reflections beyond 2.3 Å were greater than 20%, and data beyond 2.3 Å were not used in the refinement process for that reason. Reflection intensity data to 2.3 Å were 99.7% complete with an average of five observations per reflection.

Molecular Replacement. Solution of the structure by rotation and translation, using programs and procedures described previously (Bystroff et al., 1990), was accomplished in a straightforward manner. The starting model was the protein part of the refined holoenzyme. The rotation function calculation yielded the expected six symmetry-related peaks at 5.9σ to 5.1σ above background with the highest nonsolution peak 0.5σ lower than the lowest solution peak.

The translation function, CBT1, written by one of us and documented elsewhere (Bystroff, 1988; Crowther & Blow, 1967), was run with data from 4.5 to 7.0 Å and both possible space groups, $P3_121$ and $P3_221$. As for the ternary complex reported previously, the space group ambiguity was resolved when one space group, $P3_121$, produced a 5.6σ peak while the enantiomeric space group produced no peaks higher than 4.0σ . The solution peak was 1.4 Å thick at half-height and was confirmed by a local R factor search which gave a minimum R factor of 45%. The rotated and translated protein part of the holoenzyme coordinates was the starting model for least-squares refinement.

Refinement. Least-squares structure factor refinement was carried out as previously described (Bystroff et al., 1990). After initial refinement of the molecular replacement solution using CORELS (Sussman et al., 1977), we employed PROLSQ (Hendrickson, 1985) during the rest of the refinement process. A liquid solvent correction factor was incorporated in the calculation throughout refinement according to the method introduced by Bolin et al. (1982). Residues 16–20, missing in the molecular replacement search model, were omitted from the initial coordinate set. As no density was observed for this chain segment during the course of refinement, it is also omitted from the refined structure. Changes in R factor and geometry during refinement generally stopped after three to five cycles. After each round of refinement, we used the programs FRODO (Jones, 1978) and MMS (Dempsey, 1987) to inspect the model and to make changes where necessary.

Refinement was stopped after 70 cycles when further calculations produced no significant improvements in either the R factor or the geometry. Aside from the exceptions discussed under Results, the final electron density maps did not suggest any significant further changes in the model. Areas that are still not fully interpreted or understood are discussed under Results.

Manipulation of Models. The α -carbon coordinates for all of the available DHFR models were superimposed on the holoenzyme structure with the program OVRLAP (Rossmann & Argos, 1975). The holoenzyme was chosen as the reference structure because of its low average temperature factor (22 Å²) and its backbone conformation, which was found to be intermediate between the conformations of the apoenzyme and the MTX binary complex. We see no significant difference in the relative positions of the α -carbons if we choose a different reference structure.

The magnitude and axial orientations of the relative domain rotations within the molecule were determined by successive independent superposition of the two domains of each structure onto the reference structure—in this case, the apoenzyme. With one domain superimposed on the corresponding domain of the apoenzyme, the rotation and translation required to

² Touch seeding refers to the method in which a fiber (hair or glass) is used to touch a protein crystal and then a suitably prepared drop of protein solution in order to transfer a small number of submicroscopic crystal nuclei.

least-squares superimpose the other domain with the apoenzyme was considered to be the relative domain rotation between the given structure and the apoenzyme. The magnitude of the relative domain rotation is defined as the angular absolute value of this operation, and the coordinates of the axis of the rotation were extracted as the eigenvector of the rotation/translation operator.

Distance Difference (ΔD) Plots. Two-dimensional $\text{C}\alpha$ – $\text{C}\alpha$ distance plots, introduced by Ooi and Nishikawa (1973), have been used to identify domains within a protein molecule (Go, 1983). In this study we use ΔD plots, which show differences between two $\text{C}\alpha$ – $\text{C}\alpha$ distance plots, as an unbiased description of the conformational changes between two structures of the same molecule. ΔD plots allow easy identification of regions of the molecule which behave as rigid bodies as well as floppy loop regions.

Each point on a distance difference plot has the value

$$\Delta D(i,j) = D_1(i,j) - D_2(i,j)$$

where $D_1(i,j)$ is the distance between the α -carbons of residues i and j in structure 1, $D_2(i,j)$ is a similar measurement in structure 2, and $\Delta D(i,j)$ is the difference between them. The ΔD values are plotted in a square matrix with i on one axis and j on the other. Because $D(i,j) = D(j,i)$ the array of ΔD values is mirror symmetrical about the diagonal. In Figure 1 positive values have been contoured in the lower right triangle and negative values have been contoured in the upper left triangle. The contour levels are ± 0.50 , ± 1.50 , and ± 2.25 Å.

RESULTS

Apoenzyme Refinement. A total of 70 cycles of PROLSQ refinement lowered the R factor to 19.8% for data between 20 and 2.3 Å. Standard deviations from ideal geometry are, for bond lengths, 0.026 Å and, for planar groups, 0.024 Å. The average B factor is 31 Å², with a standard deviation of 12 Å². Main-chain atoms have an average B factor of 28 Å², side chains 30 Å², and water molecules 51 Å². The average electron density at atomic positions in a $2F_o - F_c$ map is 1.8σ above the mean value for the map. For backbone atoms the average density is 2.1σ above the mean, for side chains 1.8σ , and for waters 0.8σ . The overall RMS error in atomic position, as estimated by the method of Luzzati (1952), is 0.25 Å.

Disordered Regions. The regions of the apo-DHFR molecule that are absent, weak, or possibly inadequately modeled after 70 cycles of refinement are as follows: residues 16–20 are missing; residues 21–24 are weak; there is uninterpreted extra density associated with the Phe-31 side chain; residues 95–96 are partially disordered. Val-10, Glu-120, Asp-122, and Asp-127 have disordered side chains. The side chain of Leu-28, in the substrate binding site, seems to be partially disordered.

We regard the present structure as refined not to "completion" but to a point where only certain discrete portions require further attention. For analysis of backbone conformational changes the structure is more than adequate. Aside from the regions discussed below, our present model for the apoenzyme fits the $2F_o - F_c$ electron density very well.

A possible explanation for the extra density on the Phe-31 side chain is that it represents a partially disordered phthalate molecule since the crystals were grown in phthalate buffer. Phthalate may bind weakly in the hydrophobic PABG-binding cleft. We have tentatively modeled the extra density using water molecules.

Residues 16–20 of the Met-20 loop were found to be disordered, as expected from the holoenzyme structure, and are

not included in the apoenzyme coordinate set. Throughout the refinement process we searched the Met-20 loop area for contiguous density but found none. The backbone density terminates at the same positions as seen in the holoenzyme, that is, at the carbonyl of Gly-15 and at Pro-21(N). We believe, therefore, that the disorder seen at the Met-20 loop in the holoenzyme structure reported in our previous paper is neither unique to that complex nor due to that particular crystal packing but rather that it is characteristic of the *E. coli* DHFR molecule when its folate binding pocket is unoccupied. Residues 21–24, Pro-Trp-Asn-Leu, are partially disordered in the apoenzyme, with high B factors (40–50 Å²) and poorly defined density which is broken between residues 23 and 24. In the empty PABG and nicotinamide binding regions, discontinuous positive difference electron density, which does not have the usual appearance of spherically shaped water peaks, may indicate that the nearby Met-20 loop partially occupies those sites. Model-building experiments show that such a chain conformation for the Met-20 loop is possible.

95–96 Peptide, Cis or Trans? Glycines 95 and 96 in the previously reported *E. coli* DHFR structures, and the equivalent invariant glycine pair in the *Lactobacillus casei* and chicken DHFR structures, form a cis peptide bond; but in the *E. coli* apoenzyme the Gly–Gly peptide bond may flip between a cis and a trans conformation. The 95–96 region in both the ternary complex and the holoenzyme is well ordered, with well-defined density and relatively low temperature factors (about 10 Å² in the holoenzyme, 30 Å² in the ternary). In the apoenzyme, however, the backbone chain density diminishes at N and C α of Gly-96, giving a pinched appearance to the contoured map, and the density for the adjacent 96–97 (also Gly–Gly) peptide clearly indicates that the carbonyl oxygen of Gly-96 should be directed 180° away from where it was initially modeled. This adjustment causes the carbonyl oxygen to protrude into the binding pocket for the cofactor's pyrophosphate rather than allowing it to hydrogen bond to the backbone nitrogen of Tyr-100. On the basis of "omit" maps and the results of parallel refinement cycles in which we modeled the 95–96 peptide bond in both the cis and trans conformation, our interpretation is that the 95–96 peptide bond is disordered, being partially cis and partially trans. No attempt was made to refine the relative occupancy of cis and trans conformers, but the refined trans conformer fits the density somewhat better than the cis. Therefore, the backbone has been modeled as a trans peptide at 95–96 for the present.

Our tentative conclusion is that the 95–96 peptide switches between the cis and trans conformations. This conformational switch may account for the slow interconversion of the unliganded enzyme between an active form and a form that binds neither NADPH nor dihydrofolate (Baccanari & Joyner, 1981; Cayley et al., 1981; Penner & Frieden, 1985). Clearly, with the Gly-96 oxygen protruding into the pyrophosphate binding site as it does in the trans 95–96 conformation, NADPH could not bind productively. But it is not obvious how a possible cis/trans isomerization might affect the binding of dihydrofolate.

Packing Interactions. Lattice contacts in the apoenzyme crystals appear to be weak solvent-mediated or ionic interactions. No extended contacts were observed, in contrast to the folate-NADP⁺-DHFR ternary complex or the MTX binary complex (Bystroff et al., 1990). The lattice contacts do not block the active site, nor do they involve any of the residues which take part in substrate or coenzyme binding, with the sole exception of a van der Waals contact with His-45, which hydrogen bonds to the pyrophosphate moiety of NADP⁺.

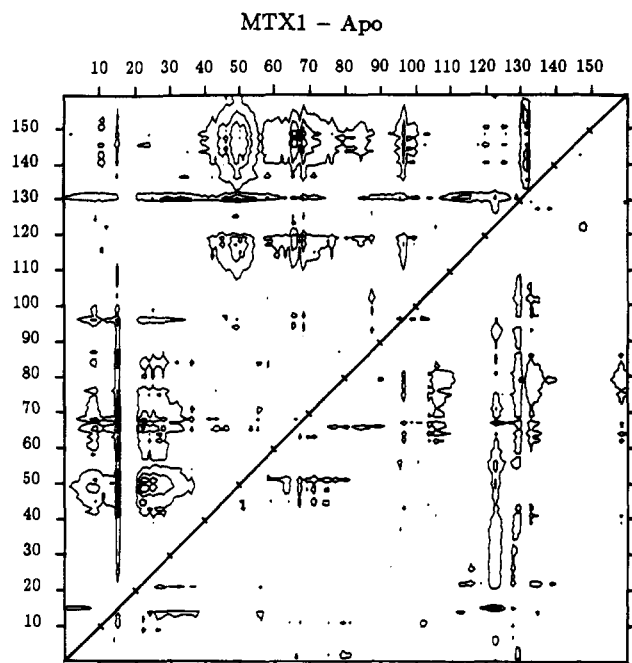


FIGURE 1: Example of distance difference (ΔD) plot for comparison between α -carbon positions of two *E. coli* DHFR crystal structures, in this case the MTX binary complex minus apoenzyme. Positive values are contoured at 0.5, 1.5, and 2.25 Å in the lower right triangle. Negative values are contoured at 0.5, 1.5, and 2.25 Å in the upper left triangle. Typical features of these plots are described in the text.

Analysis of Conformational Differences. Conformational differences between the five *E. coli* DHFR structures were analyzed by use of distance difference (ΔD) plots and least-squares superposition statistics, as well as, of course, visual inspection on a graphics station.

We employed ΔD plots as an unbiased measure of conformational changes, not depending on how molecules are superimposed. Figure 1 is an example of a ΔD plot used in the conformational analysis. It shows typical features that reappear in several pairwise comparisons. For example, an overall look at the plot reveals a predominance of negative over positive values, indicating that the first structure (the MTX binary) is more compact than the second (the apoenzyme). It would be difficult to make such an assessment only on the basis of visual comparison of the two molecular models. By inspecting the ΔD plots, we found that the ternary complex and the MTX binary were more compact than the holoenzyme or the apoenzyme, although in each pairwise comparison the changes occurred in different places. Large differences were also evident between the ternary and the MTX binary, but there was no indication of overall shrinkage. Likewise, the apoenzyme and the holoenzyme are the same in overall size, but ΔD plots indicate that they differ in shape.

Besides overall size differences, there are two distinctive types of features that can be identified in a ΔD plot—streaks and blocks. A streak indicates that a series of residues moved relative to the rest of the molecule. Thus, they may constitute a floppy loop. A more-or-less rectangular block, or blob, of difference values indicates that the residues involved are parts of two rigid domains. Rigid domains maintain constant distance relationships within their boundaries but move in relation to each other. Thus, distance differences are large primarily between residues in different rigid groups and not within such a group.

More detailed analysis of a ΔD plot involves identifying rigid domains that rotate relative to each other. A relative domain rotation might move one part of a domain closer to and another

part farther away from a second domain, producing blocks of positive values and blocks of negative values. Residues within the two domains that show no changes are near the axis of rotation.

Figure 1, comparing the apoenzyme and the MTX binary complex, shows that DHFR has two rigid substructures: one consisting of approximate residue numbers 1–37 and 89–159 and the other of residues 38–88. These two rigid substructures we refer to as the “major domain” (1–37, 89–159) and the “adenosine binding domain” (38–88). Use of the term “domain” here is not meant to imply any hypothesis about whether or not they constitute folding units. Other pairwise comparisons reveal that a relative domain rotation also occurs on going from the apoenzyme to each of the other liganded complexes. Between each pair of liganded complexes a relative domain rotation of lesser and varying magnitude is observed.

INTERPRETATIONS AND DISCUSSION

With the structure of *E. coli* apo-DHFR reported here and with the existing structures of the holoenzyme, MTX binary complex, and folate-NADP⁺ ternary complex, we now have an *E. coli* DHFR structure for every combination of liganded and unliganded binding sites. [This is the second crystal structure of an unliganded DHFR molecule. A 3.0-Å refinement of the chicken apoenzyme has been completed but not yet fully analyzed—S. J. Oatley, unpublished data.] In this section we present a dynamic model for *E. coli* DHFR, dividing the molecule into substructures and describing how they move relative to one another. We will then describe how changes in the enzyme conformation are induced by the binding of ligands, either MTX or NADP⁺ to the apoenzyme or folate to the holoenzyme, and how these conformational changes may provide a structural basis for cooperativity in binding. Finally, we will ask whether the conformation of DHFR in the MTX binary complex may resemble its conformation in the transition state.

A Simplified Conformational Dynamics Model: Two Domains. For purposes of describing ligand-induced conformational changes in the enzyme molecule, *E. coli* DHFR can be thought of as composed of two domains. Residues 1–37 and 89–159 constitute the larger or major domain and residues 38–88 the smaller adenosine binding domain (see Figure 2). The division into domains was determined by a consensus of information from distance difference plots, superposition statistics, and visual analysis of the internal clustering of hydrophobic side chains. The boundary between domains cuts across the PABG binding site, the pyrophosphate site, and the adenine binding site. It should be emphasized that, as used here, a domain is simply a group of residues that approximates a rigid body in its dynamic behavior. The idea that the domains defined here are in some sense “folding units” was not considered, although such a possibility cannot be ruled out.

The major domain contains that portion of the central β -sheet comprising β -strands G, H, F, A, and E, and α -helices B and F (see Figure 2). The secondary structural elements of the major domain, except for αB , behave as a unit exhibiting few internal conformational changes among the five structures; αB is more mobile. Between the β -sheet and αF there is a large cluster of hydrophobic side chains, including six Leu's (4, 8, 104, 110, 112, 156), two Tyr's (100, 128), two Phe's (103, 125), two Val's (93, 99), Trp-133, Ile-2, and two Ala's (6, 107). The surface-facing side of αF contains many polar side chains, giving the helix an amphipathic character and fixing it tightly to the surface of the β -sheet. Another smaller cluster of hydrophobic residues is found on the opposite side of the β -sheet between the sheet and αB . This core consists

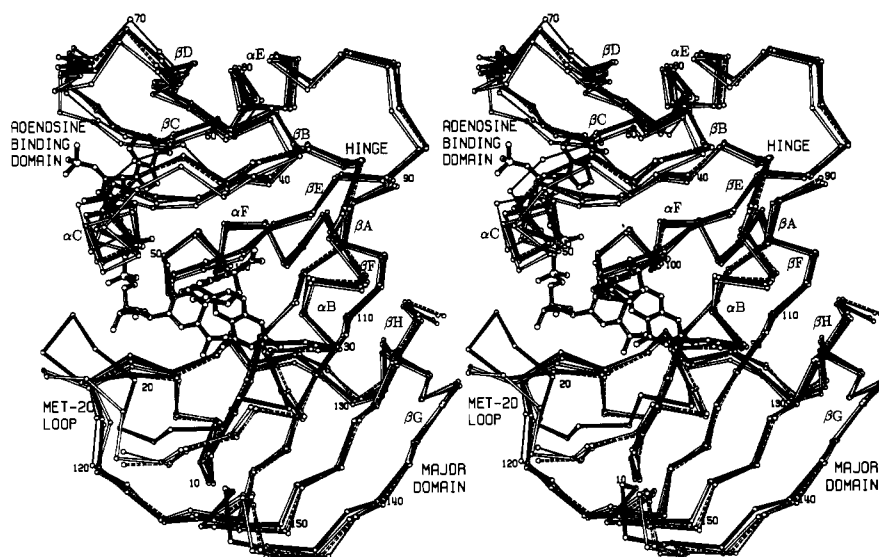


FIGURE 2: α -Carbon backbone representations of apo-DHFR (thin lines), the oxidized holoenzyme (dashed bonds), the folate-NADP⁺ ternary complex (filled bonds), and the methotrexate binary complex (open bonds) superimposed by least squares. NADP⁺ (striped bonds) and folate (thick filled bonds) are shown as they bind in the ternary complex. Secondary structures and the proposed domains have been labeled. The adenosine binding domain consists of residues 38–88, and the major domain consists of the remaining N-terminal and C-terminal sequences. The “Met-20 loop” is the β A– α B connecting loop. The label “hinge” identifies the two backbone chain connections between domains.

of the side chains of Ile-5, Trp-30, Met-92, Tyr-111, Phe-137, Tyr-151, Phe-153, and Ile-155. Most likely because both clusters of hydrophobic side chains are anchored to the β -sheet, they behave as a single rigid unit. Most of the major domain exhibits very little variance between the five DHFR structures, as evidenced by distance difference plots and least-squares superposition statistics. Exceptions to this rule are the α B helix and the floppy connecting loops between elements of secondary structure. The motions of α B and the connecting loops will be discussed later.

The adenosine binding domain (ABD) contains β -strands B, C, and D and α -helices C and E. A small hydrophobic cluster, composed of Met-42, Trp-47, Ile-61, Val-72, and Trp-74, lies between α C and the β -sheet. These residues maintain a constant spatial relationship to each other as the adenosine binding domain rotates relative to the major domain. The coenzyme and the substrate (or inhibitor) bind in the crevices between the two domains, except for the adenosine ribose and the 2'-phosphate of the coenzyme, which bind exclusively to the ABD.

The Hinge Region. The two backbone-chain connections between the adenosine binding domain and the major domain are the short connections α B– β B and α E– β E. It is interesting to note that these two short connecting loops are the loci of two of the largest insertions in the sequences of vertebrate DHFR's according to the sequence alignments in Volz et al. (1982). This agrees with the findings of others [reviewed by Neurath (1986)] that insertions and regions of low homology occur in the hinges between domains. These observations, and the rigid-body behavior of the two domains described above under Results, suggest that the covalent connection between the domains is relatively unimportant for their function. Rather, the noncovalent interactions—hydrogen bonds and hydrophobic contacts in the region between β -strands B and E (see Figure 2)—determine the interdomain flexibility.

The noncovalent interactions that hold the molecule together tend to be weaker in the domain/domain interface than in the core of the domains. β -Strands B and E interact via only three consecutive backbone hydrogen bonds, fewer than any other adjacent pair of β -strands in the molecule. A β -bulge at Ile-94 prevents the formation of a fourth consecutive hydrogen bond.

There is a backbone hydrogen bond between Gly-95(O) and Gly-43(N) following the β -bulge, but it is distorted.

Hydrophobic side chains make contact across the domain/domain interface on both sides of the axis of rotation, the side that opens and the side that closes. Met-42 and Val-40 of the ABD interact with Met-92 and Ile-94 of the major domain on one side of the axis, whereas Ile-41 interacts with Val-93 on the other side. These contacts, like the interdomain hydrogen bonds between β B and β E, do not significantly restrict the relative domain rotation because they are close to the rotation axis. Other hydrophobic contacts between domains exist which are located a greater distance from the axis of rotation and thus do restrict it. These contacts are Leu-62, Val-78, and Ile-82 of the ABD with Ile-2, Ile-91, and Phe-103 of the major domain. Some of these residues form the adenine binding site.

Relative Domain Rotations. As implied by the title of the preceding section, the conformational changes of *E. coli* DHFR seen on comparison of the crystal structures can be described in a first approximation as a hinge motion of one domain relative to the other. The motion is restricted to a rotation of one domain about an axis approximately halfway between β -strands B and E; the range of the rotation is about 6 deg, with the extreme open conformation occurring in the apoenzyme and the extreme closed conformation in the MTX binary complex, molecule 1. For the purposes of this discussion, the “open” conformation is the one in which the PABG binding site is wider, and the “closed” conformation is the one in which that site is relatively constricted. The apoenzyme is in the open conformation whereas the MTX binary complex is in the closed conformation. Both the holoenzyme and the ternary complex exhibit an intermediate conformation.

It should be noted that the superimposed ABD backbone atom positional differences between the holoenzyme and the ternary complex are small, usually within the error in the latter structure, and therefore, we may say that the holoenzyme and the ternary complex have essentially the same relative domain-rotational conformation.

As seen in Figures 3 and 4, the axis of rotation is not completely fixed; i.e., the “hinge” has some play in it, reflecting the fact that the analogy of two domains and their relative

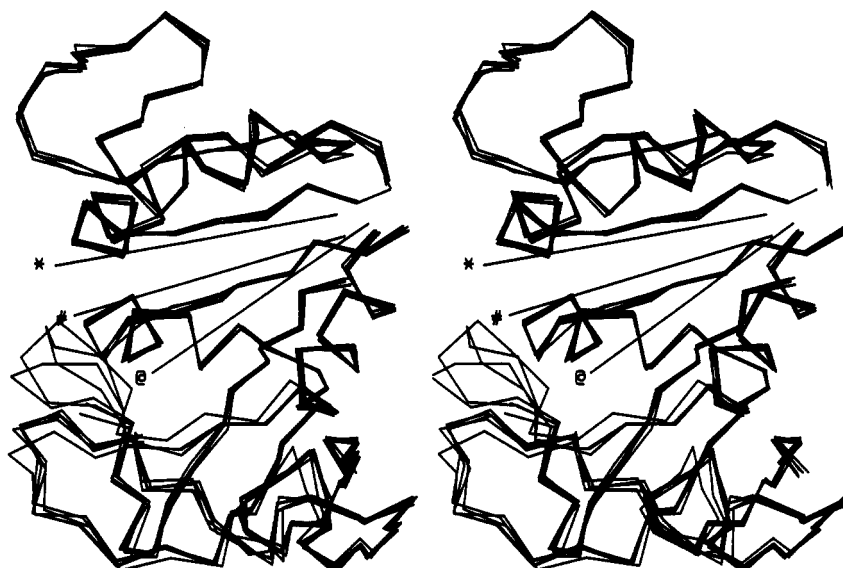


FIGURE 3: Superimposed α -carbon backbones of the adenosine binding domain (upper portion) and the major domain (lower portion) separately superimposed by least squares on the backbone of the apoenzyme. The straight lines represent the approximate eigenvectors of the difference between the superposition operators for the major domain and the adenosine binding domain. The eigenvector is equivalent to the rotation axis for the conformational change between domains for (*) holoenzyme to apoenzyme, (#) methotrexate binary complex (molecule 2) to apoenzyme, and (@) methotrexate binary complex (molecule 1) to apoenzyme. Axis (*) also represents the rotation axis for folate-NADP⁺ ternary complex to apoenzyme. The rotations are approximately 4.5° for the holoenzyme (*) or ternary complex, 7° for MTX binary molecule 2 (#), and 6° for MTX binary molecule 1(@).

rotation is only a crude approximation to the enzyme molecule's conformational dynamics. In Figure 3 one can see that the three observed positions for the domain-rotation axis, calculated as described under Materials and Methods, nearly intersect in the region of the hinge but take significantly different directions. This means that there is a certain amount of "pivot" character to the hinge. Figure 4 shows the α backbones of the various complexes of *E. coli* DHFR superimposed with the apoenzyme. Each view is down the axis of rotation for the pair of structures indicated. The location of the rotation axis determines the extent to which the domain rotation alters each binding site.

Table I gives some representative distance differences across the adenine, pyrophosphate, and PABG binding sites. Note that the distances across the NMN and pteridine binding sites are affected by the shift of α B and the Met-20 loop as well. The primary effect of the domain rotation from the apoenzyme to each of the liganded complexes is to close the hydrophobic PABG-binding cleft between α B and α C. Additionally, the closing motion shrinks the pyrophosphate binding site, which lies between the N-termini of α -helices C and F. The same domain rotation also opens, slightly, the hydrophobic adenine binding pocket, but the degree to which it opens depends on the location of the domain-rotation axis.

Hinge Motions and Exposed Hydrophobic Surfaces. The relative domain rotation that closes the PABG-binding cleft when ligands are bound also opens the hydrophobic adenine binding site. In the absence of ligands, this motion would expose a greater hydrophobic surface area to solvent, which appears to be energetically unfavorable and may explain why the apoenzyme molecule is in the open conformation. In complexes containing the cofactor, the adenine ring apparently would shield its binding site from solvent and thus make opening of that site less unfavorable. Also, van der Waals contacts between the adenine moiety and the walls of the binding site would evidently prevent the site from closing. As a result, in the holoenzyme and the ternary complex the PABG-binding cleft would be predicted to assume a more closed conformation than in the apoenzyme (see Figure 5d,f).

Table I: Change in Internal Dimensions of Binding Sites for Various Moieties of Folate and NADP⁺, Relative to Their Sizes in the Apoenzyme^a

binding site and atom	atom	difference distance (Å): apo to			
		holo	ternary	MTX1	MTX2
pyrophosphate					
R98(N)	H45(C)	-0.7	-0.9	-0.5	-0.5
2'-phosphate					
S64(N)	R44(C α)	+0.5	+0.2	+0.4	+0.3
R44(C)	Q65(N)	+0.7	+0.5	-0.1	-0.3
adenine					
K76(O)	R98(C α)	+1.2	+1.0	-0.1	+0.6
S64(N)	Q102(C α)	+0.1	+0.6	-0.7	+0.0
NMN ribose					
T46(N)	G15(C α)	+0.4	-0.3	(-2.2) ^b	-1.3
nicotinamide					
T46(C α)	A7(N)	+0.3	+0.1	-1.1	-0.8
I94(O)	I14(O)	+0.2	-0.1	(+1.6) ^b	-1.1
pteridine					
I94(O)	D27(O δ 1)	+0.7	+0.9	-0.4	-0.3
I5(O)	L28(C δ 2)	-1.3	-1.8	-1.3	-1.4
L28(C δ 2)	F31(C δ 1)	-0.2	-0.6	-0.3	+0.1
p-aminobenzoate					
L28(C δ 2)	I50(C α)	-0.6	-1.2	-1.9	-1.6
W22(N ϵ 1)	L54(C δ 2)	-0.0	-0.5	-0.8	-0.8
glutamate					
L28(C α)	P55(N)	-0.4	-0.3	-0.6	-0.9

^a Abbreviations: apo, apo-DHFR; holo, NADP⁺-DHFR holoenzyme complex; ternary, folate-NADP⁺-DHFR ternary complex; MTX1 and MTX2, methotrexate binary complex, molecules 1 and 2; NMN, nicotinamide mononucleotide. ^b In MTX1, I14 is flipped and G15 occupies the empty NMN site.

A similar domain rotation occurs on going from the apoenzyme to the MTX binary complex, even though the cofactor is absent (see Figure 4). This can be rationalized by observing that in the MTX binary complex the axis of rotation shifts noticeably toward the adenine binding site, diminishing the effect of the domain rotation on the size of the adenine binding site. Furthermore, in the MTX binary complex the unfavorable exposure of hydrophobic surfaces to solvent at the adenine site may be compensated by the burying of hydrophobic side chains on binding the PABG group of MTX.

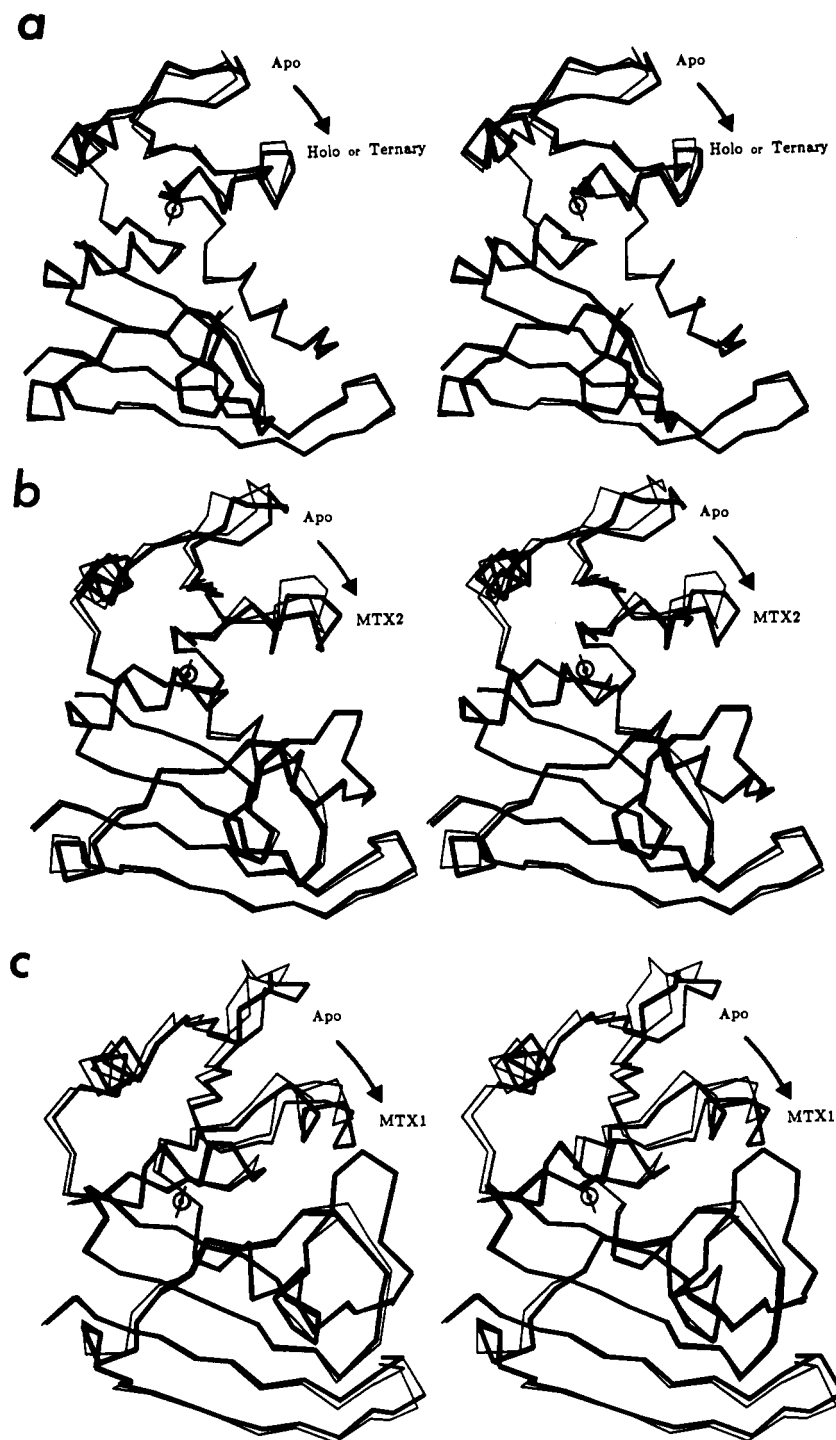


FIGURE 4: Least-squares superimposed structures of the apoenzyme (thin lines) and (a) the holoenzyme, (b) the MTX binary complex, molecule 2, and (c) the MTX binary complex, molecule 1 (all thick lines). Each view looks directly down the least-squares axis for the relative rotation of the adenosine binding domain induced by NADP^+ or MTX binding. Arrows indicate the direction of the rotation. The holoenzyme conformation also approximately represents the folate: NADP^+ ternary complex with regard to this conformational change.

Movements in the Floppy Loop Region. In a simple two-domain dynamic model, if we consider the main core of the major domain to be fixed, there are only two portions of the *E. coli* DHFR molecule that move substantially. We have already discussed the relative rotation of the adenosine binding domain. The other mobile portion of the molecule is the floppy loop region of the major domain. Movement of this region interacts with movement of the αB helix. It comprises three flexible loops—the Met-20 loop (9–23) connecting βA and αB , the loop connecting βF and βG (117–131), and the loop connecting βG and βH (142–149)—and constitutes about one-third of the major domain. But the three loops do not

behave as a rigid body. Rather, the loop region serves as a gate or lid, closing over the bound ligands in the ternary complex but remaining mobile in the apoenzyme, the holoenzyme, and probably also in the MTX binary complex. More specifically, the Met-20 loop folds over the binding sites for the pteridine and NMN moieties, while the other two loops perform supporting roles in this conformational change.

In the apoenzyme and holoenzyme crystal structures, the central part (16–20) of the Met-20 loop (9–23) is disordered. In the MTX binary complex crystal structure those residues are involved in a lattice interaction and thus are ordered, but assume two very different conformations (recall that there are

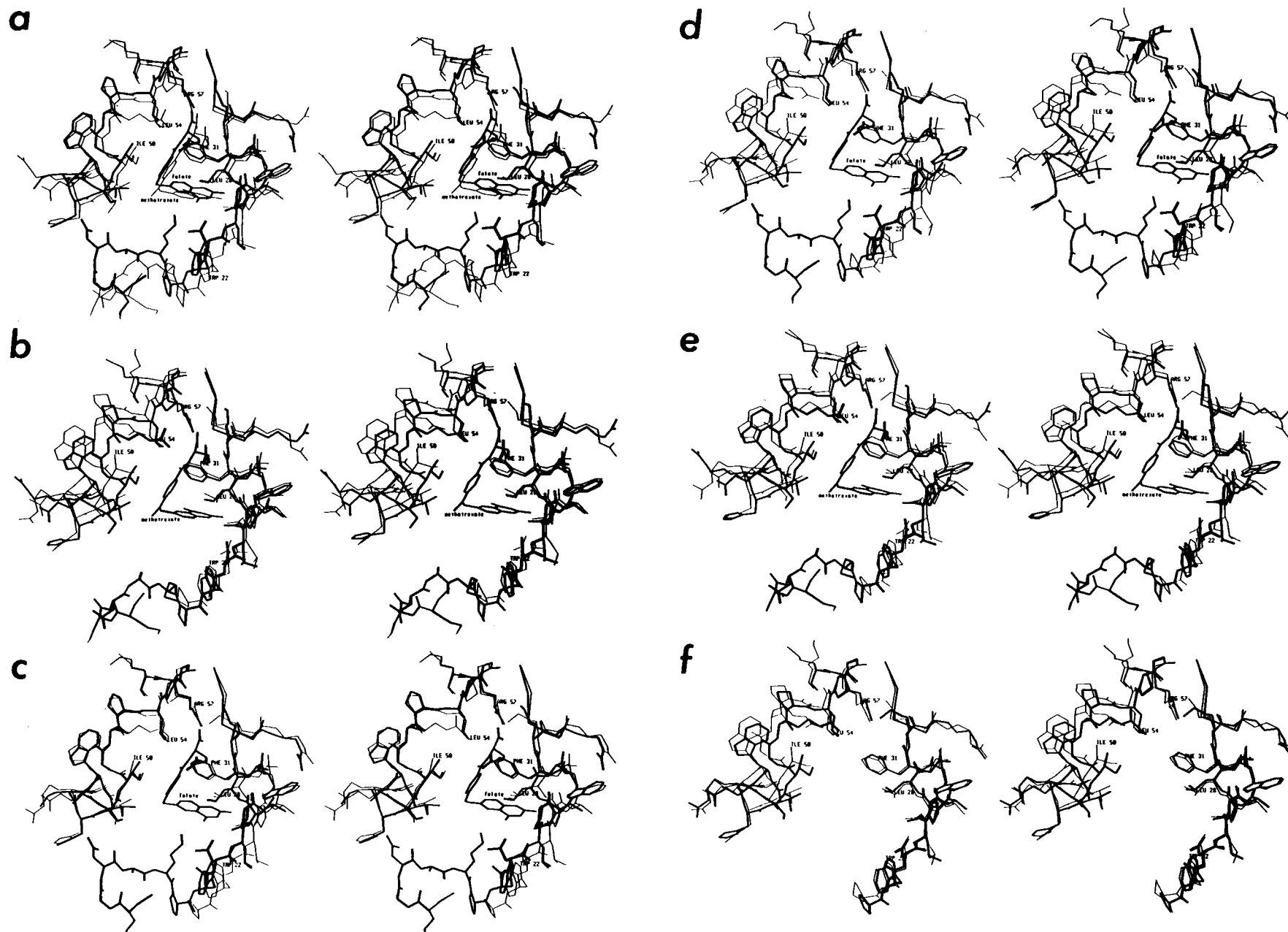


FIGURE 5: Pairwise comparisons among the four structures (utilizing only molecule 1 of the MTX binary complex) at the (*p*-aminobenzoyl)glutamate- (PABG) binding cleft: (a) MTX binary (thin lines), folate-NADP⁺ ternary (thick lines); (b) apoenzyme (thin lines), MTX binary (thick lines); (c) holoenzyme (thin lines), ternary (thick lines); (d) apoenzyme (thin lines), ternary (thick lines);

(e) holoenzyme (thin lines), MTX binary (thick lines); (f) apoenzyme (thin lines), holoenzyme (thick lines). NADP⁺ is not shown. Illustrated is the ability of the PABG-binding gap to close from either side. Least-squares superpositions were calculated with all α -carbons.

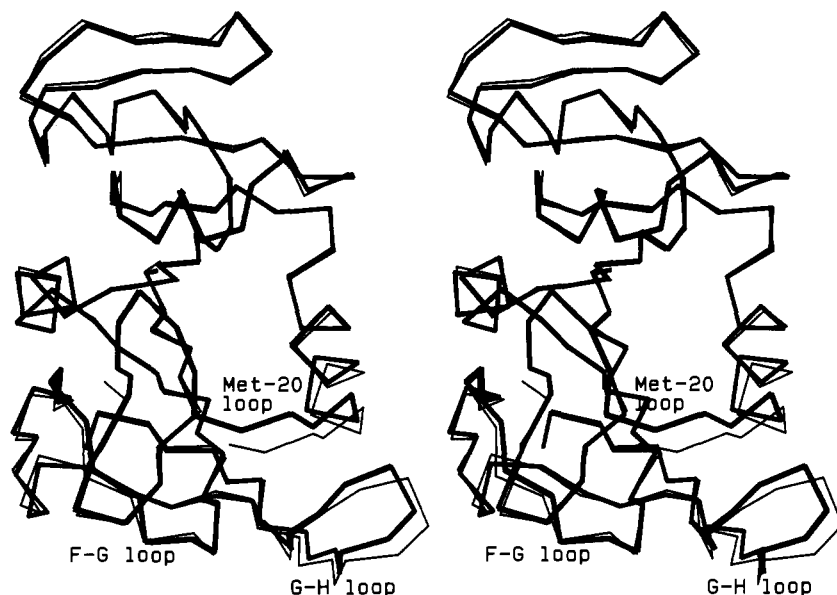


FIGURE 6: The loop region of the major domain. The holoenzyme (thin lines) is superimposed with the folate-NADP⁺ ternary complex (thick lines). The missing section of the Met-20 loop in the holoenzyme comprises the disordered segment 16–20. Also illustrated here is the bending and rolling of the α B helix (to the right of the Met-20 loop) on going from the holoenzyme to the ternary complex.

two molecules in the asymmetric unit). Evidently the binding of neither NADP⁺ nor MTX alone causes the Met-20 loop to become ordered, but it becomes ordered in the presence of both substrate and coenzyme. In so doing it pinches into a type I hairpin turn defined by a hydrogen bond between the backbone carbonyl of Met-16 and the backbone NH of Ala-19 and folds over the NMN and pteridine binding sites (see Figure 6). The Asn-18 side chain makes a hydrogen bond across the gap to the backbone carbonyl of His-45 on α C. The loops β F– β G (117–131) and G–H (142–149) respond to the more compact folding of the Met-20 loop by collapsing toward the latter.

Bending of the α B Helix. In the ternary complex the α B helix bends toward the pteridine binding site, paralleling the shift of the Met-20 loop (see Figure 6). An 8°–10° rotation of α B about an axis perpendicular to the helix near its C-terminus (residue 35) and subtle distortions of its hydrogen-bonding geometry along most of its length result in displacement from the apoenzyme conformation of about 1.5 Å at the N-terminus of α B. The slightly distorted helix has longer hydrogen bonds on the side facing away from the pteridine and shorter hydrogen bonds on the side facing the pteridine. Leu-24, at the N-terminus of α B, rotates so that its carbonyl oxygen appears to hydrogen bond to both Asp-27(N) and Leu-28(N), suggesting that the first turn of the α B helix is becoming a 3_{10} helical turn in the ternary complex. In addition to the observed bending α B also rolls roughly 10° counterclockwise, as viewed down the helix axis from the N- to C-terminus, when compared with the holoenzyme (see Figure 6).

In the MTX binary complex the α B helix has shifted about 0.6 Å toward the pteridine binding site from its position in the apoenzyme. But in this case α B shifts by means of a rigid-body translation rather than by bending and rolling. As a result of the α B shift observed in the ternary complex, contacts between residues 21–24 and the β G– β H loop are lost. Of the four hydrogen bonds present in the holoenzyme, three are lost, and one is distorted in the ternary complex. This loss appears to be an energetic penalty for the α B shift. But model-building studies suggest that formation of the hairpin turn at residues 16–19 is not possible without a significant shift in residues 21–24, so the energetic penalty may be coupled to the energetic

bonus of the hairpin turn formation.

NADP⁺-Induced Conformational Changes in the Apoenzyme. NADP⁺ binding to the apoenzyme induces a 4.5° relative domain rotation (see Figure 4a), thereby improving hydrogen bonding with the pyrophosphate moiety. Figure 7 illustrates how the pyrophosphate interacts with the α F and α C helices at their respective N-termini. The α C helix shifts from a position in the apoenzyme where the backbone nitrogens of His-45 and Thr-46 would be too far away (about 3.8 Å each) from the oxygens of the pyrophosphate to make good hydrogen bonds. In the holoenzyme the new backbone hydrogen-bond distances are still rather long (3.6 and 3.2 Å), but the α C helix shift also improves the geometry of the bifurcated hydrogen bond from the His-45 side chain to the pyrophosphate. Moreover, the Thr-46 side chain moves 1 Å closer to the pyrophosphate and allows a hydrogen bond from the side chain of Thr-46 that would otherwise not be possible. The domain rotation also redirects the positive end of the α C helix dipole such that it lies closer to the negative charges of the pyrophosphate. Model building suggests that a slightly greater domain rotation would further improve these hydrogen bonds and would move the positive end of the helix dipole still closer to the pyrophosphate. One possible explanation for why this does not happen may be that, in addition to improving those interactions, a greater domain rotation would also separate the hydrophobic side chains of Leu-62 and Val-78 in the ABD from those of Val-99 and Phe-103 in the major domain.

The 2'-phosphate moiety of NADP⁺ binds between the β C– β D loop and α C of the adenosine binding domain. As is also the case for the adenine binding site, the 2'-phosphate binding site in the apoenzyme is too small to accommodate the coenzyme. In the holoenzyme the somewhat floppy β C– β D loop has moved to open a space. At the same time as the ABD rotates to open the adenine binding site, the β C– β D loop moves in the opposite direction, resulting in a small net change in position relative to the major domain but increasing the distance across the 2'-phosphate binding site (see Table I). It is interesting to note that coenzymes and coenzyme analogues lacking the 2'-phosphate show negative cooperativity with dihydrofolate binding, whereas coenzymes and analogues having the 2'-phosphate show positive cooperativity (Stone et al., 1984). This finding may point to the α C helix as the

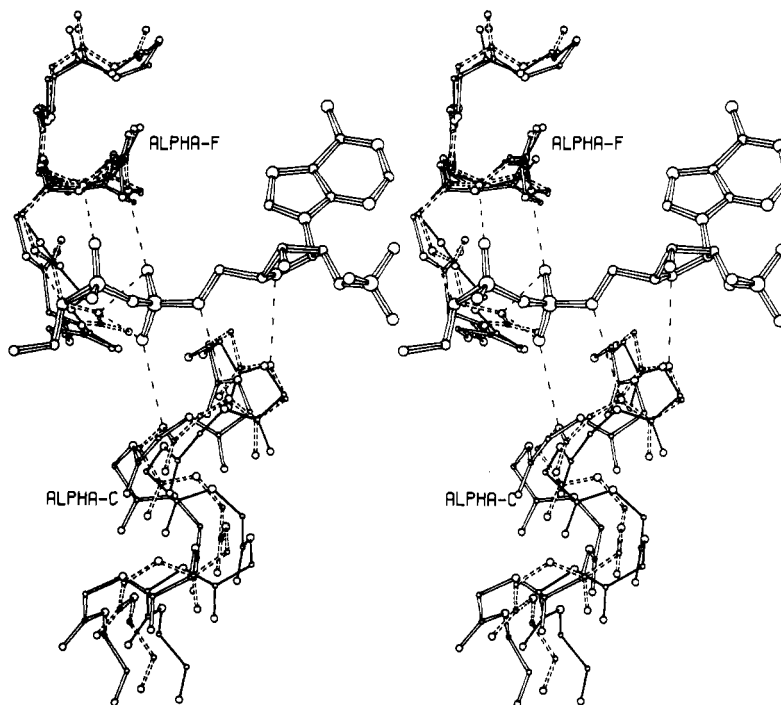


FIGURE 7: Interactions of the backbones of α -helices F (above) and C (below) with the pyrophosphate moiety of NADP⁺ (striped bonds). The apoenzyme (thin lines), holoenzyme (dashed bonds), and the MTX binary complex (open bonds) are superimposed. The figure shows that α F is relatively immobile, whereas α C shifts from its conformation in the apoenzyme to form hydrogen bonds with the pyrophosphate in the holoenzyme. In the MTX binary complex α C is shifted farther in the same direction, but also slightly downward. Superpositions were calculated by least squares with all α -carbons.

mediator of cooperativity, since that is the only mobile substructure of DHFR that interacts with both the 2'-phosphate and the substrate (specifically, the PABG moiety). Possibly, α C does not shift as much unless the 2'-phosphate is inserted between it and the β C- β D loop. We proposed previously that the 2'-phosphate serves as an anchor, fixing the conformation of the ribose (Bystroff et al., 1990).

MTX-Induced Changes in the Apoenzyme. MTX binding causes a general "tightening" of the enzyme as described under Results. Table I and Figure 1 show the general decrease in distances within the molecule and across binding sites. Although the adenine site and the 2'-phosphate site are not made significantly smaller, the pyrophosphate site and the PABG cleft shrink by about 0.5 and 2.0 Å, respectively, upon binding of the inhibitor (see Figures 5b and 7). These changes are primarily the result of a 6° relative domain rotation. α B also shifts by about 0.5 Å but does not bend or roll, nor is hydrogen bonding with the β G- β H loop disrupted as in the ternary complex.

The impetus for the ABD rotation can be assigned to the binding of the PABG moiety of MTX in the gap between the side chains of Ile-50 and Leu-28. This hydrophobic gap closes by more than 2 Å upon binding of MTX to the apoenzyme (see Table I and Figure 5b). The closing motion buries the side chains of Leu-28, Phe-31, Ile-50, and Leu-54 against the PABG tail, forming a new hydrophobic cluster.

As can be seen in Figure 5, the PABG gap can close from either side—by means of a domain rotation on one side or by bending the α B helix on the other. Comparing the MTX binary complex with the apoenzyme (Figure 5b), we find that the PABG-binding cleft has closed mainly by way of the domain rotation. The α B helix has shifted by only about 0.5 Å and shows none of the bending seen in the ternary complex.

Modeling suggests that MTX could also fit into the conformation of the enzyme seen in the folate-NADP⁺ ternary complex where the domains are rotated less and α B is shifted

more (see Figure 5a). In fact, crystals of the MTX-NADP⁺ ternary complex are isomorphous with those of the folate-NADP⁺ ternary complex (Bystroff et al., 1990), making it very likely that the enzyme conformations are the same. The question arises then as to why we do not see the α B shift in the MTX binary complex, if it occurs in the MTX-NADP⁺ ternary complex. Part of the answer may be that the presence of NADP⁺ blocks the domain rotation because, as mentioned earlier, in the apo-to-MTX rotation the adenine binding pocket does not open (see Table I), whereas in the apo-to-holo rotation the adenine site does (and must) open.

The contribution of the pteridine moiety of MTX to the domain rotation is to draw the two sides of the pteridine binding site closer together. Formation of a hydrogen bond from Ile-94(O) to NA4 of MTX pulls β E about 0.5 Å in the direction of Asp-27. This results in a lateral displacement of residues 87–89 at the hinge between the domains (upper right corner of Figure 2), which in turn alters the position of the rotation axis. The domain rotation axis is shifted closer to the adenine binding site (see Figure 3), and the rotation therefore does not cause the separation of hydrophobic side chains that, as mentioned earlier, occurs there in the NADP⁺-induced domain rotation. By this argument, in the absence of the 4-amino group of MTX we would expect a different domain rotation—one that opens the adenine binding site. These structural arguments that the PABG moiety and the 2,4-diaminopteridine both contribute to the conformational change corroborate the findings of Birdsall et al. (1978), who measured binding cooperativity between fragments of the MTX molecule, namely, PABG and 2,4-diaminopyrimidine.

Folate-Induced Changes in the Holoenzyme. The most obvious conformational changes on going from the NADP⁺ binary to the ternary complex are ordering of the NMN moiety, ordering of residues 16–20 in the Met-20 loop, and a shift of α B. These changes all occur in the flexible loop region of the molecule and are quite obvious. A more subtle

change is the shift of Ile-94 away from the pteridine binding site—a result of steric crowding between the pteridine and the backbone carbonyl of Ile-94. But there is essentially no change in the relative orientation of the two domains.

With regard to the domain orientations, we may ask why there is no further rotation of the ABD when folate binds to the holoenzyme. More precisely, we want to know why the enzyme molecule chooses to shift α B rather than rotate the ABD in order to close the PABG-binding crevice. The energetically unfavorable consequences of the shift of α B were described earlier, and modeling suggests that a slightly greater domain rotation would improve hydrogen-bonding distances between α C and the pyrophosphate moiety of NADP⁺ (see Figure 7). But a larger domain rotation and smaller α B shift would alter the conformation of the PABG tail with respect to the pteridine, putting it at a more acute angle than we actually see in the ternary complex. In turn, a more acute angle between the pteridine and *p*-aminobenzoyl rings appears to be unfavorable because it would require shortening an already short 3.1-Å van der Waals contact between the pteridine C6 and *p*-aminobenzoyl C15 atoms [see Figure 7a of Bystroff et al. (1990)]. For this reason, evidently, a larger domain rotation does not occur in the ternary complex, and closing of the PABG crevice is accomplished instead by a shift of α B (see Figure 5c). In contrast to folate, MTX is not restrained by a close C6 to C15 contact because it binds with its pteridine ring turned over, and consequently, a larger domain rotation is indeed observed in the MTX binary complex.




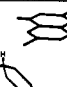

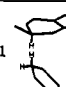
Folate binding to the holoenzyme induces ordering of the NMN moiety of the coenzyme and residues 16–20 of the Met-20 loop. In the holoenzyme structure (Bystroff et al., 1990) the NMN appears to be rotationally disordered about the P–O5' bond, and the presence of a bound folate molecule would block such a rotation. Locking the NMN into its binding site in turn provides potential interactions between the NMN ribose and the hairpin turn of the Met-20 loop, promoting formation of the latter. A hydrophobic contact between Met-20 and the pteridine ring may also contribute to ordering of the Met-20 loop.

An unfavorably close van der Waals interaction between C7 of the pteridine ring and the carbonyl oxygen of Ile-94 causes the latter to move away from the pteridine binding site. We had previously identified this interaction as possibly promoting an upward puckering at C7 and downward puckering at C6 in the 7,8-dihydropteridine ring of substrate, which ought to favor binding of the transition state. Ile-94(O) shifts approximately 0.8 Å from its position in the holoenzyme upon binding of folate, minimizing the steric clash with C7. But comparing the Ile-94 conformation in the ternary complex with its conformation in the other complexes and the apoenzyme suggests that in the ternary complex it is at the limit of its conformational flexibility.

Cooperativity in Binding. On the basis of the existing crystal structures, *E. coli* DHFR appears to have two ways in which it can change its conformation and thereby change the shape of its binding sites: (1) the relative domain rotation and (2) the shifts within the loop region. In this section, we will attempt to correlate the domain rotation with thermodynamically observed positive cooperativity in binding. Whether conformational changes in the loop region contribute to either positive or negative cooperativity is unclear.

Binding of either NADP⁺ or MTX appears to induce a similar domain-closing rotation. On the basis of model building, one can argue that folate, too, would induce such a rotation. Hence, we predict positive cooperativity between the

Table II: Cooperativity in Binding (K_{coop}) as a Function of the Choice of Pteridine Ligand (P) and Coenzyme (C)^a

	K_{coop}	P		
		MTX	DHF	THF
C	NADP ⁺	12.5 	2.4 	0.6 
	NADPH	680 	0.5 	0.01 

^a Of interest is the crowding or lack thereof at the point of contact between C6 of the pteridine (DHF or THF) and C4 of the coenzyme. Values were calculated from published dissociation constants (Birdsall et al., 1978, 1981a,b; Cayley et al., 1981; Dunn et al., 1978; Dunn & King, 1980; Poe, 1977). Abbreviations: MTX, methotrexate; DHF, 7,8-dihydrofolate; THF, 5,6,7,8-tetrahydrofolate. $K_{\text{coop}} = K(E \cdot P + C \rightleftharpoons E \cdot P \cdot C) / K(E + C \rightleftharpoons E \cdot C) = K(E \cdot C + P \rightleftharpoons E \cdot C \cdot P) / K(E + P \rightleftharpoons E \cdot P)$.

coenzyme and either MTX or folate. Our reasoning is as follows: We deduce that there is an intrinsic energetic cost associated with the domain-closing rotation in the absence of ligands. If this were not so, we would have expected to see the apoenzyme in the closed conformation instead of the open conformation actually observed. (We assume, of course, that the conformation of the enzyme in the crystal is essentially the predominant conformation in solution, remaining aware as always of the possibility that crystal lattice interactions affect the protein conformation. But as stated earlier, the lattice interactions are weak and therefore less likely than the comparatively strong ligand binding interactions to cause significant conformational changes.) When both ligands are bound, the first will bear the energetic cost of the conformational change, and the second will not, giving positive cooperativity. On the other hand, in the ternary complex we have a close contact between C4 of the nicotinamide ring of NADP⁺ and C6 of the pteridine of folate [discussed in Bystroff et al. (1990)], which suggests that these parts of the two ligands compete for the same space. By itself this close contact would contribute to *negative* binding cooperativity. Furthermore, as hydrogen atoms are added to C4 and C6 van der Waals crowding ought to increase and so too its contribution to negative cooperativity.

One can see this predicted effect by examining trends in cooperativity as crowding at the C4–C6 contact increases. Table II gives some values for cooperativity in binding MTX, dihydrofolate, or tetrahydrofolate and reduced or oxidized coenzyme. Cooperativity becomes more negative ($K_{\text{coop}} < 1$) as hydrogens are inserted between C4 and C6 and crowding increases. Note particularly that MTX, with its pteridine ring inverted, avoids unfavorably close contact with the nicotinamide. Instead of negative cooperativity, we see positive cooperativity ($K_{\text{coop}} > 1$) in binding of MTX and NADP⁺ or NADPH. Part of this positive cooperativity is probably due to MTX and the coenzyme completing each other's binding sites. But an additional contribution to positive cooperativity probably results from the fact that the same domain rotation is induced by binding of either ligand. This idea is supported by the observation that positive cooperativity also occurs between dihydrofolate and analogues of the coenzyme (such as ADP-ribose) which lack the groups that interact directly (Stone et al., 1984).

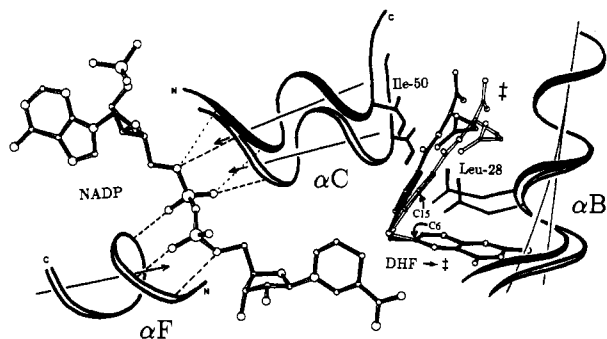


FIGURE 8: Hypothetical conformational change in the transition state. The PABG tail bends to the right, allowing αB to straighten and inducing a shift of αC . The αC shift in turn improves hydrogen bonds to the pyrophosphate of NADPH and directs the positive end of the helix dipole closer to the oxygens of the 5'-phosphate. αF serves to rigidly fix the position of the pyrophosphate. The black representations of αB and αC show their observed positions in the folate-NADP⁺ ternary complex, whereas the white representations show their positions in the MTX binary complex and in the hypothetical transition-state complex. The position of αF is the same in both cases. Labels indicate the positions of C6 and C15 of the substrate, a strained contact.

Possible Conformational Changes in the Transition State.

In our previous paper (Bystroff et al., 1990), we mentioned that a close contact between C15 and C6 of the substrate could favor the transition state for hydride transfer by promoting pyramidalization of C6. Figure 8 illustrates a hypothetical conformational change that could take place while approaching the transition state. As C6 is pyramidalized, the close contact between C15 of the PABG and C6 of the pteridine is relieved. The contact distances between the enzyme and the PABG are shorter on the Ile-50 side than on the Leu-28 side, suggesting that the enzyme wants to move the PABG toward Leu-28. And because the only interaction obviously hindering such a shift in the folate-NADP⁺ ternary complex is the C15-C6 close contact, we have attempted to model the transition state with the PABG moving toward Leu-28 in the αB helix. As the PABG shifts, so do αB and αC to accommodate it. αB returns to its unbent conformation as seen in the apoenzyme, the holoenzyme, and the MTX binary complex and regains hydrogen bonds to the βG - βH loop. Thus an unfavorable conformation of αB in the ternary complex is relieved in the transition state. The shift of αC may improve hydrogen-bond distances from the N-terminus of that helix to the pyrophosphate moiety of NADP⁺ and redirect the positive end of the helix dipole closer to the center of negative charge on the pyrophosphate. Not shown are possible improvements in hydrogen bonding between Asp-27 and the pteridine ring resulting from the αB shift, discussed in the transition-state modeling section of our previous paper. An impression derived from these model-building experiments is that a slightly larger domain rotation would also favor the transition state.

Does the MTX Complex Resemble the Transition State?

The extremely tight binding of MTX to DHFR has led us to speculate as to whether the inhibitor may in some way resemble a transition-state analogue. In fact, we can point to two ways in which the MTX complex does structurally resemble the model for the transition-state complex proposed above. First, the inverted binding mode of the MTX pteridine ring causes the target position for hydride transfer (C6 in the folate-NADP⁺ ternary complex) to be left vacant, and therefore both MTX and NADPH can bind optimally without the unfavorably close contact between the nicotinamide and the pteridine rings. Strained binding interactions in the folate-NADP⁺ ternary complex that are caused by this close contact will be relieved in the MTX complex, which will thus

more nearly resemble the transition state. A second way in which the MTX complex may resemble the transition state is with respect to the position of its PABG moiety. We proposed above that in the transition state the PABG of the substrate shifts toward αB , accompanied by a shift of the αB helix and the adenosine binding domain. All of these modeled conformational shifts resemble those actually observed in the MTX binary complex. In short, MTX may be likened to a transition-state analogue inasmuch as the conformation of the enzyme in the MTX complex probably resembles that in the transition-state complex.

CONCLUSIONS

Ligand-induced conformational changes in *E. coli* DHFR can now be described in precise structural terms on the basis of comparisons among five crystallographically independent views of the enzyme molecule in four different ligation states. A new structure of apo-DHFR has allowed us to correlate binding interactions with changes in conformation. The two major conformational changes observed are (1) a relative domain rotation of 4°–7° between the adenosine binding domain (residues 38–88) and the major domain (residues 1–37 and 89–159) and (2) a shift of helix B accompanied by reordering of three loops in a region at the N-terminus of αB . The domain rotation closes down the binding sites for the NADPH pyrophosphate and the PABG moiety, while opening the adenine binding site when the cofactor is present. One of the three loops, the Met-20 loop (residues 9–20), forms a new hairpin turn which folds over the NMN and pteridine binding sites in the folate-NADP⁺ ternary complex. The pyrophosphate and the PABG appear to play the most important roles in inducing the domain rotation, the pyrophosphate through hydrogen bonding and charge interactions with αF on one side and αC on the other and the PABG through hydrophobic interactions with αC on one side and αB on the other. Measured values for cooperativity in binding between MTX, dihydrofolate, or tetrahydrofolate and reduced or oxidized coenzyme support our structural arguments that (1) positive cooperativity results from a domain rotation induced by binding of either the PABG moiety of the substrate, the coenzyme, or both and (2) negative cooperativity arises from an unfavorably close contact between the substrate and coenzyme.

The pteridines of folate and MTX induce different conformational changes owing to the inverted orientation of the latter in the binding pocket. MTX binding rotates the domains more than either NADP⁺ alone or than NADP⁺-folate. We suggest that MTX complexes, either binary or ternary, resemble the proposed transition-state conformation (Bystroff et al., 1990) because of the shifted position of its PABG moiety relative to that of folate and because its inverted pteridine avoids steric crowding with the nicotinamide ring if the cofactor is present. In the absence of steric crowding, the nicotinamide and pteridine rings can assume their most favored binding geometries, as they would in the transition state. A conformational shift toward that seen in the MTX binary complex might stabilize the transition state for hydride transfer relative to the ground state by improving hydrogen bonding to the pyrophosphate as well as by relieving strained interactions in the loop region.

ACKNOWLEDGMENTS

We thank Prof. N. H. Xuong for use of his X-ray data collection facilities and the San Diego Supercomputer Center for a generous grant of CPU time.

Registry No. DHFR, 9002-03-3; NADP, 53-59-8; MTX, 59-05-2; folate, 59-30-3.

REFERENCES

- Appleman, J. R., Howell, E. E., Kraut, J., Kuhl, M., & Blakley, R. L. (1988) *J. Biol. Chem.* 263, 9187-9198.
- Appleman, J. R., Howell, E. E., Kraut, J., & Blakley, R. L. (1990) *J. Biol. Chem.* 265, 5579-5584.
- Baccanari, D. P., & Joyner, S. S. (1981) *Biochemistry* 20, 1710-1716.
- Birdsall, B., Burgen, A. S. V., Miranda, J. R., & Roberts, G. C. K. (1978) *Biochemistry* 17, 2102-2110.
- Birdsall, B., Burgen, A. S. V., Hyde, E. I., Roberts, G. C. K., & Feeney, J. (1981a) *Biochemistry* 20, 7186-7195.
- Birdsall, B., Gronenborn, A., Clore, G. M., Roberts, G. C. K., Feeney, J., & Burgen, A. S. V. (1981b) *Biochem. Biophys. Res. Commun.* 101, 1139-1144.
- Bolin, J. T., Filman, D. J., Matthews, D. A., Hamlin, R. C., & Kraut, J. (1982) *J. Biol. Chem.* 257, 13650-13662.
- Bystroff, C. (1988) Ph.D. Thesis, University of California, San Diego, La Jolla, CA.
- Bystroff, C., Oatley, S. J., & Kraut, J. (1990) *Biochemistry* 29, 3263-3277.
- Cayley, P. J., Dunn, S. M. J., & King, R. W. (1981) *Biochemistry* 20, 874-879.
- Crowther, R. A., & Blow, D. M. (1967) *Acta Crystallogr.* 23, 544-548.
- Dempsey, S. (1987) *Molecular Modeling System (MMS)*, Department of Chemistry Computer Facility, University of California, San Diego, La Jolla, CA.
- Dunn, S. M. J., & King, R. W. (1980) *Biochemistry* 19, 766-773.
- Dunn, S. M. J., Batchelor, J. G., & King, R. W. (1978) *Biochemistry* 17, 2356-2364.
- Filman, D. J., Bolin, J. T., Matthews, D. A., & Kraut, J. (1982) *J. Biol. Chem.* 257, 13663-13672.
- Go, M. (1983) *Proc. Natl. Acad. Sci. U.S.A.* 80, 1964-1968.
- Hendrickson, W. A. (1985) *Methods Enzymol.* 115, 252-270.
- Jones, T. A. (1978) *J. Appl. Crystallogr.* 11, 268-272.
- Luzzatti, V. (1952) *Acta Crystallogr.* 5, 802-810.
- Neurath, H. (1986) *Chem. Scr.* 27B, 221-229.
- Ooi, T., & Nishikawa, K. (1973) in *Conformation of Biological Macromolecules and Polymers* (Bergman, E., & Pullman, B., Eds.) p 173, Academic Press, New York.
- Pattishall, K. H., Burchall, J. J., & Harvey, R. J. (1976) *J. Biol. Chem.* 251, 7011-7020.
- Penner, M. H., & Frieden, C. (1985) *J. Biol. Chem.* 260, 5366-5369.
- Poe, M. (1977) *J. Biol. Chem.* 252, 3724-3728.
- Rossmann, M. G., & Argos, P. (1975) *J. Biol. Chem.* 250, 7525-7532.
- Stone, S. R., Mark, A., & Morrison, J. F. (1984) *Biochemistry* 23, 4340-4346.
- Sussman, J. L., Holbrook, S. R., Church, G. M., & Kim, S.-H. (1977) *Acta Crystallogr.* A33, 800-804.
- Volz, K. W., Matthews, D. A., Alden, R. A., Freer, S. T., Hansch, C., Kaufman, B. T., & Kraut, J. (1982) *J. Biol. Chem.* 257, 2528-2536.
- Williams, J. W., Duggleby, R. G., Cutler, R., & Morrison, J. F. (1980) *Biochem. Pharmacol.* 29, 589-595.

Mechanism of Inactivation and Identification of Sites of Modification of Ornithine Aminotransferase by 4-Aminohex-5-ynoate[†]

Daniela De Biase,[†] Maurizio Simmaco,[§] Donatella Barra,[§] Francesco Bossa,[§] Michael Hewlins,^{||} and Robert A. John^{*†}

Departments of Biochemistry and Chemistry, University of Wales College of Cardiff, P.O. Box 903, Cardiff CF1 1ST, Wales, United Kingdom, and Dipartimento di Scienze Biochimiche A. Rossi Fanelli and Centro di Biologia Molecolare del Consiglio Nazionale delle Ricerche, Universita La Sapienza, 00185 Roma, Italy

Received May 24, 1990; Revised Manuscript Received November 1, 1990

ABSTRACT: The inactivation of ornithine aminotransferase by an enzyme-activated irreversible inhibitor 4-aminohex-5-ynoate was accompanied by stoichiometric binding of the radiolabeled compound. Distribution of radiolabel among separated tryptic peptides indicated that more than one amino acid residue had reacted. Lys-292 and Cys-388 were positively identified. Reduction with borohydride was necessary to stabilize the adduct formed with Lys-292, and the relevant peptide prepared after this treatment contained equimolar amounts of inhibitor and coenzyme. The coenzyme chromophore in this peptide showed strong negative circular dichroism. A mechanism consistent with these observations is proposed.

The compound 4-aminohex-5-ynoate was designed and synthesized (Jung & Metcalf, 1975) as an enzyme-activated irreversible inhibitor with the intention of selectively inactivating 4-aminobutyrate aminotransferase because of the known an-

ticonvulsant effects of raising the concentration of the inhibitory neurotransmitter 4-aminobutyrate in brain (Fowler & John, 1972; Anlezark et al., 1976). However, besides inactivating its intended target, it also inactivates several other pyridoxal phosphate dependent enzymes, notably, ornithine aminotransferase, glutamate decarboxylase, and, much more slowly, aspartate aminotransferase (Jung & Seiler, 1978; John et al., 1979). Of these enzymes, ornithine aminotransferase is perhaps the most appropriate to use in analysis of the

[†] This work was supported by Grant ST2J-0371-c(A) from the Commission of the European Communities.

^{*} Department of Biochemistry, University of Wales.

[§] Universita La Sapienza.

^{||} Department of Chemistry, University of Wales.